Biochimica et Biophysica Acta 1859 (2017) 28–39

Contents lists available at ScienceDirect

Biochimica et Biophysica Acta

journal homepage: www.elsevier.com/locate/bbamem

Structure and function of PspA and Vipp1 N-terminal peptides: Insights into the membrane stress sensing and mitigation

Christopher McDonald [a,b], Goran Jovanovic [a], B.A. Wallace [c], Oscar Ces [b], Martin Buck [a,*]

[a] Department of Life Sciences, Imperial College London, London SW7 2AZ, UK
[b] Department of Chemistry and Institute of Chemical Biology, Imperial College London, London SW7 2AZ, UK
[c] Institute of Structural and Molecular Biology, Birkbeck College, University of London, London, WC1E 7HX, UK

ARTICLE INFO

Article history:
Received 20 July 2016
Received in revised form 18 October 2016
Accepted 27 October 2016
Available online 30 October 2016

Keywords:
Anionic lipids
Stored curvature elastic stress
Peripheral membrane protein
Amphipathic helix conformation
Membrane structure

ABSTRACT

The phage shock protein (Psp) response maintains integrity of the inner membrane (IM) in response to extracytoplasmic stress conditions and is widely distributed amongst enterobacteria. Its central component PspA, a member of the IM30 peripheral membrane protein family, acts as a major effector of the system through its direct association with the IM. Under non-stress conditions PspA also negatively regulates its own expression via direct interaction with the AAA+ ATPase PspF. PspA has a counterpart in cyanobacteria called Vipp1, which is implicated in protection of the thylakoid membranes. PspA's and Vipp1's conserved N-terminal regions contain a putative amphipathic helix a (AHa) required for membrane binding. An adjacent amphipathic helix b (AHb) in PspA is required for imposing negative control upon PspF. Here, purified peptides derived from the putative AH regions of PspA and Vipp1 were used to directly probe their effector and regulatory functions. We observed direct membrane-binding of AHa derived peptides and an accompanying change in secondary structure from unstructured to alpha-helical establishing them as *bona fide* membrane-sensing AH's. The peptide-binding specificities and their effects on membrane stability depend on membrane anionic lipid content and stored curvature elastic stress, in agreement with full length PspA and Vipp1 protein functionalities. AHb of PspA inhibited the ATPase activity of PspF demonstrating its direct regulatory role. These findings provide new insight into the membrane binding and function of PspA and Vipp1 and establish that synthetic peptides can be used to probe the structure-function of the IM30 protein family.

1. Introduction

The cell envelope provides protection from the environment and gives structural integrity to the cell in all organisms. Homeostasis of the plasma membrane is vital for functioning of the cell and the bacterial phage shock protein (Psp) response protects the bacterial membrane under various extracytoplasmic stress conditions. Although many different stimuli trigger induction of the Psp response, the common theme is disruption of the plasma membrane and consequently loss of the (trans)-membrane potential and dissipation of the proton motive force (pmf) [1–4]. By an unknown mechanism, the Psp response rescues the proton gradient and conserves the pmf by protecting the plasma membrane integrity. The central component of the Psp system is the peripheral plasma membrane binding protein PspA belonging to the IM30 family of proteins found in many organisms. In bacteria, the Psp response and PspA-like proteins are implicated in protein translocation, virulence and resistance to antimicrobials that target the cell wall or reorganise the membrane architecture [3,5–9].

In enterobacteria, PspA is a dual function protein responsible for both the negative regulation and effector function of the Psp response. Under non-stress conditions PspA directly interacts with the subunits of the *psp* transcription activator, the hexameric bacterial enhancer binding protein PspF, imparting negative regulation by inhibiting PspF's ATPase activity and the subsequent sigma54-dependent transcription of *psp* genes [3,10]. PspA-PspF interactions occur *via* the PspF W56 loop, a surface exposed hydrophobic region on each PspF subunit [11–13]. Under inner membrane (IM) stress conditions, PspF is released from the PspA-F inhibitory complex leading to induction of the Psp response. Stresses such as defects in protein translocation systems or mislocalisation of outer membrane secretins into the IM are sensed by the IM proteins PspB and PspC [13,14] resulting in a direct interactions

Abbreviations: Psp, Phage shock protein; pmf, proton motive force; IM, inner membrane; TLE, total lipid extract; PG, phosphatidylglycerol; PS, phosphatidylserine; SCE, stored curvature elastic; AH, amphipathic helix; ITC, isothermal titration calorimetry; CD, circular dichroism; SUV, small unilamellar vesicle; DOPC, 1,2-dioleoyl-sn-glycero-3-phosphocholine; DOPG, 1,2-dioleoyl-sn-glycero-3-phospho-(1′-rac-glycerol); LUV, large unilamellar vesicle; DMPC, 1,2-dimyristoyl-sn-glycero-3-phosphocholine; DOPE, 1,2-dioleoyl-sn-glycero-3-phosphoethanolamine; DOPS, 1,2-dioleoyl-sn-glycero-3-phosphoserine; TFE, trifluoroethanol.

* Corresponding author at: Department of Life Sciences, SAFB, Imperial College London, London, SW7 2AZ, UK.
E-mail address: m.buck@imperial.ac.uk (M. Buck).

http://dx.doi.org/10.1016/j.bbamem.2016.10.018

between PspB-C and the PspA subunits of the PspA-F inhibitory complex that release PspF. The PspB-C dependent signalling is conditional and severe stresses such as extreme temperature, hyperosmotic or ethanol shock cause partial or complete PspB-C-independent induction of the Psp response [1,3,4]. Following release of PspF, the PspA binds to the IM and forms high-order oligomeric (up to 36mer) effectors complexes [13,15,16] able to repair IM damage and conserve the pmf [17] but unable to stably interact with PspF to impose negative control [18].

Characterising PspA IM-binding is key to understanding the mechanism by which PspA repairs the membrane. PspA as a high-order oligomer binds to vesicles made from *E. coli* total lipid extracts (TLE) and vesicles containing the anionic lipids phosphatidylglycerol (PG) or phosphatidylserine (PS). PspA was also shown to prevent proton leakage form *E. coli* TLE vesicles *in vitro* [17]. McDonald et al. [18] showed that both anionic lipids and accumulation of the membrane Stored Curvature Elastic (SCE) stress from type II lipids drive vesicle association of PspA. *Psp*-inducing extracytoplasmic stress stimuli may well lead to the accumulation of SCE stress and associated lipid packing defects within the IM which disrupt membrane integrity and so stimulate PspA binding. Anionic lipids promote PspA binding to vesicles with low membrane SCE stress; the higher the membrane SCE stress, the less anionic lipids contribute to membrane association [18] suggesting the SCE stress may be the primary signature of the damaged membrane to be repaired by PspA.

The N-terminal region of PspA consists of two putative amphipathic helixes (AHs) (see Fig. 1), AHb required for negative control, and AHa required for effector function [19]. The N-terminal AHa (ahA; residues 2–19) is responsible for IM binding and effector function *in vivo*. The lack of AHa or amino acid substitutions in the hydrophobic face of the helix abolishes PspA IM-binding and high-order oligomer formation *in vivo* and *in vitro*. The adjacent AHb (ahB; residues 25–42) is implicated in PspA negative control. The lack of AHb or amino acid substitution on the hydrophobic face of the helix abolishes PspA-PspF interaction and PspA negative control function but does not affect the IM-binding and effector function of PspA [19]. Notably, in the absence of PspF and lipids, PspA is able to form high-order oligomers *in vitro* [10,20] suggesting interaction with PspF *via* AHb is critical for preventing PspA to oligomerise. The conserved P25 helix-breaking residue separates AHa and AHb and is important for both the negative regulatory and effector function of PspA and thus might establish a mutually exclusive use of two AHs [19]. A monomeric PspA fragment 1–144 ($PspA_{1-144}$) is sufficient for PspF negative control, dependent upon residue E37 within the AHb. Importantly, in the crystal structure of $PspA_{1-144}$ the putative AHa region is unordered [21]. A transition from unordered-to-ordered alpha-helical structure upon membrane association would establish the region as a *bona fide* AH. If the PspA AHa is indeed a typical membrane-sensing AH, a structural transition following binding to the IM may cause the switch in function of the PspA. Indeed, a conformational change of PspA AHa upon IM interaction has been inferred from other functional and structural studies [19,21].

The PspA homologue Vipp1 which is implicated in thylakoid membrane biogenesis and protection in cyanobacteria, green algae and higher plants [22–25] also carries a putative N-terminal AHa (see Fig. 1). Notably, Vipp1 can substitute for PspA in *E. coli* [26,27] and the presence of its N-terminal region is required for binding to lipid vesicles and high-order oligomer formation [18,28]. Vipp1's functional similarity to PspA for vesicle stress recognition is high, except that the role of anionic lipids in Vipp1-membrane binding is more pronounced [18] in accordance with suggested function in thylakoid membrane fusion [29].

It appears that the interactions of the putative AH regions of PspA and Vipp1 are a critical aspect of the mechanisms by which the Psp response is regulated and IM or thylakoid membrane stress is ameliorated. However, there is currently no experimental evidence to show the direct functionality of these regions or characterise their behaviour as typical AHs. In this work we used synthetic peptides based on PspA and Vipp1 N-terminal AHs and vesicles of well-defined size and lipid composition to determine a direct AHa-membrane interaction and inhibition of PspF ATPase activity by PspA AHb. The quantifications of AHa membrane-binding and structural transition as well as its effect on vesicles stability offer novel insight to a possible mechanism of stress mitigation by the PspA and related effector complexes.

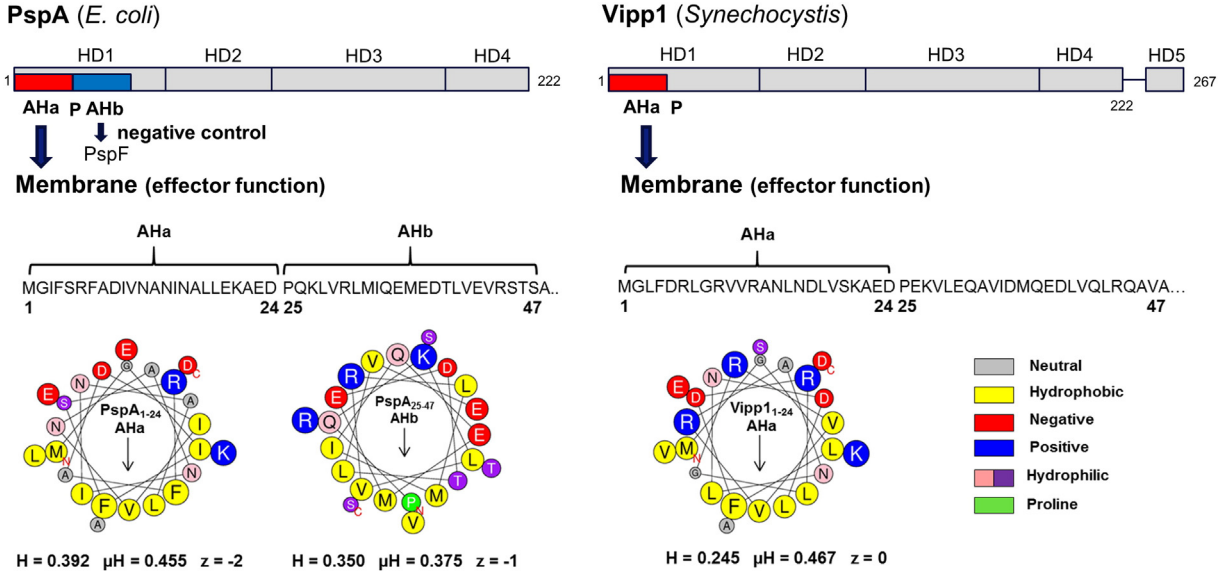

Fig. 1. N-terminal sequences of PspA and Vipp1. Schematics of PspA from *Escherichia coli* and Vipp1 from *Synechocystis* (top). Residues 1–222 of both proteins share sequence similarity and have 4 predicted alpha-helical domains labelled HD1 to HD4. Vipp1 has an extra C-terminal helical domain labelled HD5 separated from HD4 by a flexible linker region. Both proteins have an N-terminal putative AHa up to the strictly conserved P25 residue that is responsible for their membrane binding function [18,19,28]. PspA has a second putative AHb sequence after the P25 residue that causes negative regulation of PspF through interaction with the W56 hydrophobic loop [12]. The amino acid sequences and helical-wheel representations of the constitutive putative AH regions are shown below each schematic. The physiochemical parameters [50] of hydrophobicity (H), hydrophobic moment (μH) and net charge (z) are given for each AH. Arrows within each representation show the direction of the hydrophobic moment and residues are colour coded by their properties.

2. Materials and methods

2.1. Peptides

All peptides used in this study were purchased from Insight Biotechnology at ≥95% specific peptide purity (confirmed *via* HPLC and MS by the manufacturer). The peptides were supplied in powder form (including some counter ions and impurities) and the exact peptide content was determined via CHN analysis (Medac LTD) to enable preparation of peptide solutions with accurate concentrations. A table of the peptides used in this study detailing their amino acid sequences and purity is shown is Supplementary Table 2.

2.2. Preparation of lipid vesicles

Lipids were purchased from Avanti Polar Lipids (Alabastar, AL, USA). Chloroform stocks of lipids were mixed in glass vials and the chloroform was then evaporated under nitrogen. Then lipids were left in a freeze dryer overnight. Buffer was added to a 5 mM final phospholipid concentration and the suspension left above the T_M of the lipids for 1 h. The suspension was then subject to five freeze-thaw-vortex cycles. 100 nm vesicles were produced by extruding the suspension through polycarbonate filters of 100 nm pore sizes using a miniextruder (Avanti Polar Lipids). Vesicles for Isothermal Titration Calorimetry (ITC) experiments were prepared by probe sonication. All vesicles were used immediately or stored at 4 °C and used within 72 h. Vesicle sizes were characterized *via* dynamic light scattering (DLS) to ensure consistency.

2.3. Dynamic light scattering (DLS)

DLS on vesicles was undertaken as previously published (17). For measurements in the presence of $Vipp1_{1-24}$, 100 nm extruded DOPC/DOPG 6:4 vesicles (1 mM) were incubated with $Vipp1_{1-24}$ (500 μM) for 30 min before sizing.

2.4. Isothermal titration calorimetry (ITC)

Experiments were performed using a MicroCal iTC200 (Malvern Instruments Ltd). SUVs were prepared in PBS (pH 7.4). To obtain peptide binding curves, SUVs were injected into the sample cell (volume, 0.2 ml) containing peptides (in the same buffer). For experiments determining the molar enthalpy of peptide binding, peptides were injected into the sample cell containing vesicles at 25 °C. The enthalpy of dilution was determined in control experiments by injecting either peptide or vesicle samples into buffer (PBS, pH 7.4) and subtracted from the corresponding enthalpies determined in peptide-lipid binding experiments. The results were analysed using Origin software. The experiments were performed in triplicate.

2.5. Circular dichroism (CD) spectroscopy

Peptides and SUVs were dissolved or suspended in 20 mM Tris-HCl (pH 7.4). Suprasil demountable cells (Hellma UK Ltd.) with pathlengths of 0.01 and 0.005 cm were used and three spectra were collected for each sample on an Aviv 62DS spectropolarimeter over the wavelength range from 190 to 260 nm, with a 1 s dwell time at 25 °C. The replicates were averaged, and the averaged baselines (consisting of the buffer with corresponding vesicles) were subtracted from the averaged sample spectra. Data processing was carried out with CDtool software [30]. Data was analysed with the DichroWeb analysis server [31]; the reported values were the averaged results using the CONTINLL algorithm [32,33] and reference dataset 7 (chosen specifically as this reference data set includes unfolded proteins with a significant amount of unordered secondary structure). Trifluoroethanol (TFE) samples consisted of 300 μM peptide dissolved in 2,2,2-trifluoroethanol (TFE).

2.6. Calcein leakage assay

Vesicles loaded with calcein were prepared *via* extrusion of lipids hydrated in PBS pH 7.4 with 50 mM calcein (described above) followed by gel filtration through a G50 Sephadex column. Vesicles were diluted to a 1 mM lipid concentration and calcein leakage was monitored by measuring fluorescence intensity at 520 nm (excitation at 485 nm) during peptide titrations using a FLUOstar Omega microplate reader (BMG LABTECH GmbH). The experiments were undertaken in PBS pH 7.4 buffer and at 25 °C. After peptide titrations, vesicles were burst *via* addition of 0.2 M Octaethylene glycol monododecyl ether ($C_{12}E_8$) (Sigma) and fluorescence was measured to give a value for a complete dye release event. The percentage of calcein leakage was calculated according to the equation; % of calcein efflux $= (F_t - F_0)/(F_\infty - F_0) \times 100$, where F_t was the fluorescence at time t, F_0 was the fluorescence at time t_0, and F_∞ was the maximum fluorescence (100%) after the addition of $C_{12}E_8$.

2.7. Electron microscopy

Negative Stain Electron Microscopy was used to visualise the effect $Vipp1_{1-24}$ peptide had on vesicles in a calcein dye leakage assay. 3 μl samples were incubated on copper grids layered with thin carbon, washed with 3 drops of MilliQ water, and stained with 2% uranyl acetate. Images were taken on an FEI Tecnai T12 Spirit fitted with an FEI Eagle 2 K CCD.

2.8. ATPase activity

$PspF_{1-275}$WT and $PspF_{1-275}$W56A proteins were purified as described in Joly et al. [34]. The steady-state ATP hydrolysis activity of the $PspF_{1-275}$ proteins in the presence of peptides was measured using an NADH-coupled regeneration system [35]. ATPase activity was measured at 37 °C in a final volume of 100 μl containing: 25 mM Tris-HCL (pH 8.0), 100 mM KCl, 10 mM MgCl2, 1 mM DTT, 1 mM NADH, 10 mM phosphoenolpyruvate, 10 U ml^{-1} pyruvate kinase, 20 U ml^{-1} lactate dehydrogenase, 50 mM ATP, $PspF_{1-275}$ (0–5 mM) and peptides (10–500 μM). Absorbance at 340 nm was monitored every 60 s using a FLUOstar Omega microplate reader (BMG LABTECH GmbH).

3. Results

3.1. Peptide binding to small unilamellar vesicles (SUVs)

Synthetic peptides consisting of the first 24 residues of *E. coli* PspA ($PspA_{1-24}$) and *Synechocystis* Vipp1 ($Vipp1_{1-24}$) were used to probe the membrane binding properties of the putative AHa region (Fig. 1). Removal of residues 2–19 of PspA [19] and residues 1–21 of Vipp1 [28] had previously been shown to result in loss of the PspA and Vipp1 membrane binding functions. However, additional residues up to the helix-breaking P25 were included in this study as charged flanking regions have been shown to contribute to AHs membrane sensing [36] and should provide a better comparison of binding with that of the full length proteins [18]. Fig. 1 and Supplementary Fig. 1 show helical wheel projections, net hydrophobicity, hydrophobic moment and charge of the peptides used.

Isothermal titration calorimetry (ITC) was used to determine if the AHa peptides could be adsorbed from bulk solution to a phospholipid-water interface. DOPC small unilamellar vesicles (SUVs) were initially used as we observed PspA and Vipp1 binding to these neutral model membranes in previous studies [18]. The molar enthalpy of binding of $PspA_{1-24}$ and $Vipp_{1-24}$ to SUVs was determined by injecting peptide solution into a large excess of phospholipids. Due to the large excess of lipid almost all injected peptide should bind the membrane resulting in virtually identical heats for each titration. The average enthalpy measured per mole of $PspA_{1-24}$ injected was −6.6 Kcal mol^{-1} (Supplementary Fig. 2a) while the buffer control titrations resulted in an enthalpy of

-0.4 Kcal mol^{-1} (Supplementary Fig. 3a), yielding a reaction enthalpy of -6.2 (± 0.28) Kcal mol^{-1}. Injecting Vipp1$_{1-24}$ into DOPC SUVs (Supplementary Fig. 2c) resulted in a net molar enthalpy of -3.9 (± 0.18) Kcal mol^{-1} (with buffer control of 0.1 Kcal mol^{-1}, Supplementary Fig. 3b). These values imply that both PspA$_{1-24}$ and Vipp1$_{1-24}$ are able to associate with SUVs in an exothermic binding event.

Circular dichroism (CD) spectroscopy was used to examine the secondary structures of PspA$_{1-24}$ and Vipp1$_{1-24}$. Peptides tend to have low spectral magnitudes as they adopt multiple conformations in equilibrium rather than a single structure. The precise values of the calculated secondary structures determined using reference databases derived from globular soluble proteins should therefore be treated with a degree of caution, although the relative values provide valuable comparisons [37]. The CD spectra and calculated helical contents of PspA$_{1-24}$ and Vipp1$_{1-24}$ (Figs. 2a, 3a and Table 1) show that in the absence of phospholipids, both peptides were largely unstructured (~10% helical content). When DOPC SUVs (14:1 lipid to peptide -L/P- ratio) were added to PspA$_{1-24}$, a spectrum more reminiscent of a helical structure with an increased 224 nm peak was observed (Fig. 2a) and the calculated α-helix content more than doubled. For Vipp1$_{1-24}$ the spectral change was smaller (Fig. 3a) and corresponded to a ~4% increase in helix content. Although the net increase in helix content is relatively small, the CD spectra result from an ensemble of the free and bound peptide structures. Therefore the helical contents may represent either partially folded peptides in the bound state or folded bound peptides in the presence of disordered unbound peptide. The peptide-lipid binding equilibrium can be described by $P + L_c = PL_c$, where P is the peptide and L_c is the N lipids associated with the peptide [37]. The % of membrane-bound peptide, PL_c, in the CD experiments can therefore be calculated with knowledge of N and the associated macroscopic binding constant K_b [38]. To obtain these values, ITC titrations were used to derive binding isotherms (Figs. 2b, 3b and Supplementary Fig. 2b, d). PspA$_{1-24}$ was found to have $N = 76$ (± 4) DOPC molecules associated per peptide and Vipp1$_{1-24}$ had $N = 122$ (± 17). Binding constants, K_b, of 9.1×10^{-4} M^{-1} and 9.2×10^{-4} M^{-1} for PspA$_{1-24}$ and Vipp1$_{1-24}$ were obtained, respectively. Using these parameters the amounts of membrane-bound peptide in the CD samples were calculated to be 17% for PspA$_{1-24}$ and 10% for Vipp1$_{1-24}$. Thus, a large fraction of the peptides are not membrane-associated. The helicities of the membrane-bound peptides were calculated to be 78% for PspA$_{1-24}$ and 42% for Vipp1$_{1-24}$. Membrane association is clearly accompanied by significant α-helix formation in both peptides, confirming their behaviour as typical of membrane-binding amphipathic helixes.

3.2. Impact of anionic lipids on binding

Both PspA and Vipp1 proteins have increased membrane-binding capabilities in the presence of anionic lipids [18,28,29]. To determine if the AHa peptides properties are similar, SUVs containing 8:2 and 6:4 (M:M) DOPC/DOPG were used in the CD spectroscopic and ITC studies (Fig. 2b-d). For PspA$_{1-24}$, addition of anionic DOPG resulted in a change in the CD spectrum corresponding to a higher helical content compared with zwitterionic DOPC alone (Fig. 2a). DOPC/DOPG 8:2 SUVs (14:1 L/P) resulted in 34% calculated total helix content and DOPC/DOPG 6:4 SUVs (14:1 L/P) produced a further increase to 45% helicity (Table 1). ITC studies showed that this corresponded with a decrease in the number of lipid molecules per peptide binding site, N, to 39 for DOPC/DOPG 8:2 and 25 for DOPC/DOPG 6:4 (Fig. 2c, d). When this data was used to calculate the helical content of the PspA$_{1-24}$ membrane-bound fraction (as above), results very similar to those observed for DOPC SUVs were obtained (Table 1). Therefore, it appears that anionic lipids do not have a significant effect on the helicity of the membrane-bound PspA but increase the number of peptide binding sites per SUV.

In the case of Vipp1$_{1-24}$, addition of DOPG resulted in even more pronounced differences in membrane binding. Calculated total helical contents of 39% and 50% were obtained with DOPC/DOPG 8:2 and DOPC/DOPG 6:4 SUVs, respectively (Fig. 3a and Table 1). The number of lipid molecules per peptide binding site obtained from ITC studies (Fig. 3b-d and Table 1) dramatically reduce from $N = 122$ to $N = 35$ for DOPC/DOPG 8:2 and $N = 21$ for and DOPC/DOPG 6:4. 91% of the residues in membrane-bound Vipp1$_{1-24}$ were calculated to be helical for DOPC/DOPG 8:2, more than double that of DOPC. A helical content of 77% for Vipp1$_{1-24}$ bound to DOPC/DOPG 6:4 still indicated significantly more helical residues than in DOPC. DOPG therefore appears to promote further helix formation of membrane-bound Vipp1$_{1-24}$ as well as increasing the number of available binding sites on the SUVs.

For both PspA$_{1-24}$ and Vipp1$_{1-24}$ a two-fold increase in K_b is also observed when 20% DOPG is present in the membrane (Table 1) showing that the peptides have a higher affinity for membranes containing the anionic lipid. The enthalpy of reaction for PspA$_{1-24}$ binding to DOPC/DOPG 8:2 is only slightly more exothermic than to DOPC [-8.2 (± 0.22) kcal/mol *versus* -6.2 (± 0.28) kcal/mol] while for Vipp1$_{1-24}$ it

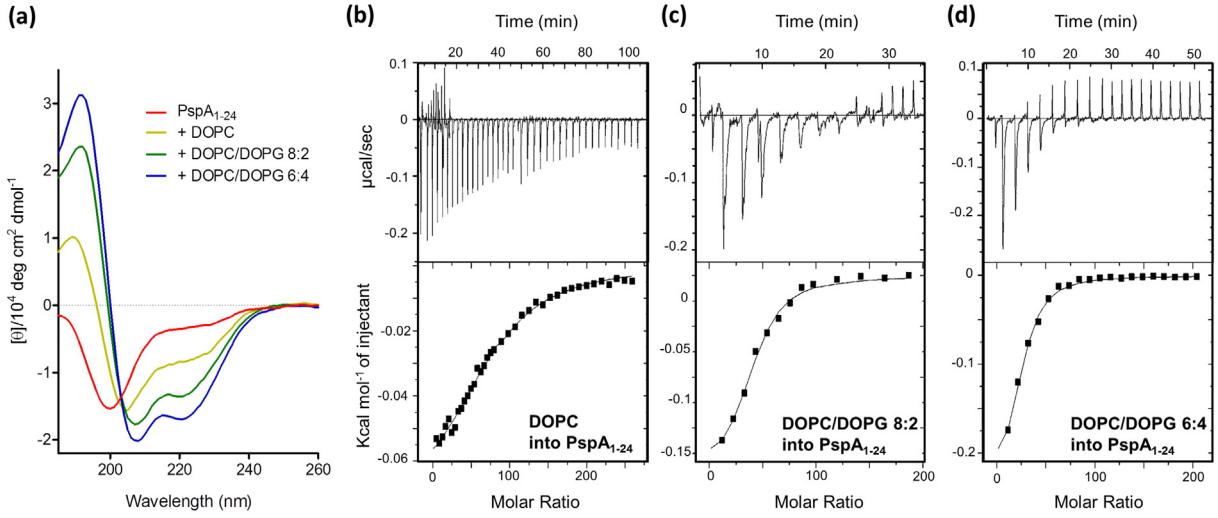

Fig. 2. Binding of PspA$_{1-24}$ to SUVs monitored *via* CD spectroscopy and ITC. (a) CD spectra of PspA$_{1-24}$ in the absence and presence of DOPC, DOPC/DOPG 8:2 and DOPC/DOPG 6:4 SUVs. Peptide concentration was 300 μM and the lipid concentration was 4.2 mM giving a 14:1 lipid to peptide ratio. (b–d) ITC tracings (top) and heat of reaction per injection number (bottom) for experiments undertaken in buffer are shown for: (b) injection of 1 μl (injections 1–20) and 2 μl (injections 21–40) aliquots of 40 mM DOPC into 50 μM PspA$_{1-24}$; (c) injections of 1.3 μl aliquots of 40 mM DOPC/DOPG 8:2 into 25 μM PspA$_{1-24}$; (d) injections of 1.3 μl aliquots of 40 mM DOPC/DOPG 6:4 into 25 μM PspA$_{1-24}$. All experiments were performed in triplicate and the raw heats shown are a representative example. The heats of dilution, measured in separate control experiments, were subtracted from the heats of reaction in each trace. The buffer controls for (b–d) are presented in Supplementary Fig. 3c–e.

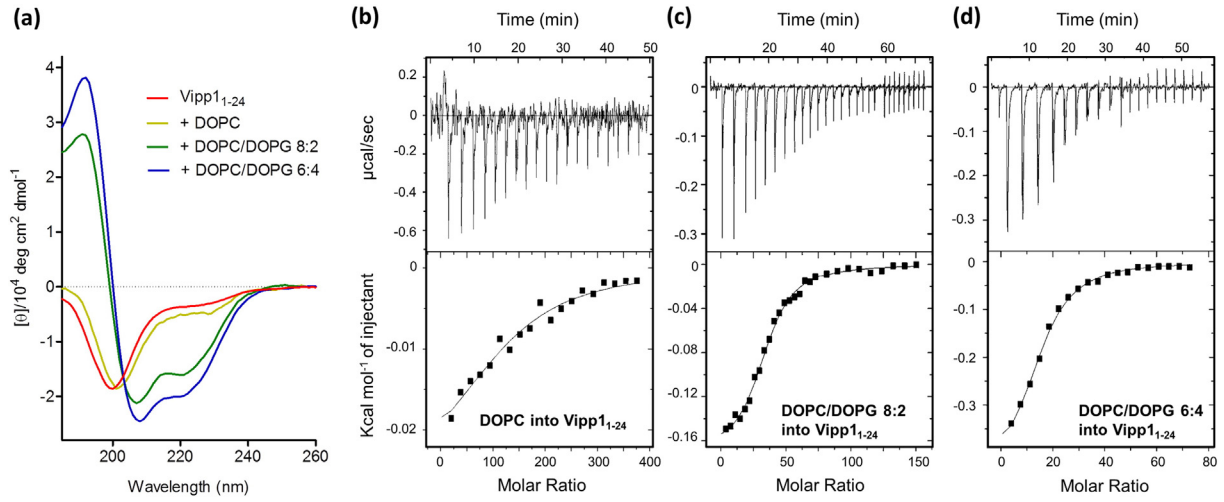

Fig. 3. Binding of Vipp1$_{1-24}$ to SUVs monitored *via* CD spectroscopy and ITC. (a) CD spectra of Vipp1$_{1-24}$ in the absence and presence of DOPC, DOPC/DOPG 8:2 and DOPC/DOPG 6:4 SUVs. Peptide concentration was 300 μM and the lipid concentration was 4.2 mM giving a 14:1 lipid to peptide ratio. (b–d) ITC tracings (top) and heat of reaction per injection number (bottom) for experiments undertaken in buffer are shown for: (b) injection of 2 μl aliquots of 40 mM DOPC into 25 μM Vipp1$_{1-24}$; (c) injections of 1.5 μl (injections 1–20) and 3 μl (injections 21–30) aliquots of 40 mM DOPC/DOPG 8:2 into 50 μM Vipp1$_{1-24}$; (d) injections of 1.5 μl aliquots of 40 mM DOPC/DOPG 6:4 into 50 μM Vipp1$_{1-24}$. All experiments were performed in triplicate and the raw heats shown are a representative example. The heats of dilution, measured in separate control experiments, were subtracted from the heats of reaction in each trace. The buffer controls for (b–d) are presented in Supplementary Fig. 3c–e.

almost doubles [−7.6 (±0.21) kcal/mol *versus* − 3.9 (±0.18) kcal/mol]. This is expected as most of the enthalpy released in AH-membrane binding interactions arises from peptide folding. Increasing the amount of anionic lipids in the membranes from 20% to 40% only appears to have a significant effect on the number of peptide binding sites while other binding parameters are largely unaffected.

3.3. CD studies with LUVs

SCE stress promotes membrane-binding of both PspA and Vipp1 proteins in an AHa-dependent manner [18]. Thus SCE stress might also affect the PspA$_{1-24}$ and Vipp1$_{1-24}$ peptides binding properties if these sequences are the major membrane binding determinants and able to function independently. Large unilamellar vesicles (LUVs) were therefore produced for the SCE stress studies. The compositions of the vesicles to test the effect of SCE stress on PspA$_{1-24}$ and Vipp1$_{1-24}$ peptides binding and structure were chosen as two extremes shown to affect the interactions of PspA and Vipp1 proteins [18]. Varying membrane SCE stress has a significant effect on the helical content of PspA$_{1-24}$ (Fig. 4a and Supplementary Table 1). The low SCE stress vesicles (LUVs composed of DMPC/DOPC 4:6) caused a slight helical increase of 3% as determined from the CD spectra of PspA$_{1-24}$. However, the high SCE stress vesicles (DOPE/DOPC 4:6) had a larger effect with helix content increasing by 15%. The addition of DOPC LUVs containing 40% anionic DOPG or DOPS resulted in increases in calculated helical contents of 13% and 19%, respectively (Fig. 4b and Supplementary Table 1). The LUVs with high SCE stress increased the helicity of Vipp1$_{1-24}$ by 6% (Fig. 4c and Supplementary Table 1) suggesting a lower level of AH mediated binding than PspA$_{1-24}$. Notably, LUVs containing DOPC alone also had an effect on the structure of PspA$_{1-24}$ and Vipp1$_{1-24}$ peptides (Supplementary Fig. 4a). Although the lipid to peptide ratio slightly differs to the DOPC/DOPE and DOPC/DMPC LUVs, preventing direct comparison, empirically the effect appears to lie somewhere between that of the LUVs possessing the two extremes of SCE stress. A large increase in helical content of Vipp1$_{1-24}$ is observed upon addition of DOPC LUVs with 40% mole fraction anionic lipid content (increase of 27% with DOPG and 38% with DOPS) (Fig. 4d and Supplementary Table 1). The use of two different anionic lipid species (DOPG and DOPS) may rule out any specific head group interactions mediating AH formation, hence, the effect of anionic lipids on PspA$_{1-24}$ and Vipp1$_{1-24}$ AHs are likely due to electrostatic interactions. It might be that, rather than exclusively SCE stress, the individual negative charge present within PE in DOPE/DOPC LUVs could trigger the interactions of PspA$_{1-24}$ peptides as well. However, although formally possible this is less likely since Vipp1$_{1-24}$, whose interactions are strongly triggered with anionic lipids, in this case was clearly less responsive than PspA$_{1-24}$.

The Vipp1$_{1-24}$ peptide binding to lipids and accompanying increase in helical structure is sensitive to the amount of anionic lipids: a gradual increase in the LUVs anionic lipid content using 10%, 20%, 30% and 40% mole fractions of DOPG resulted in a corresponding increase in the net helical content of Vipp1$_{1-24}$ at a 14:1 L/P ratio (Supplementary Fig. 4b

Table 1
Parameters of membrane-binding of PspA$_{1-24}$ and Vipp1$_{1-24}$. [a] Δ*H* are directly measured binding enthalpies estimated from peptide into lipid titrations.[b] The single macroscopic binding constants K_b were derived using the model described in the text.[c] The number of lipid molecules per peptide binding site *N* were also derived using the model described in the text.[d] Total helicity refers to the net α-helix content of peptides incubated with SUVs at a 14:1 lipid-to-peptide ratio.[e] NRMSD is a goodness-of-fit parameter between the data and calculated structures.[f] Bound helix content is the calculated percentage of residues in an **α**-helix conformation when the peptide is membrane-bound. N/A, not applicable.

Peptide	SUV composition	[a]ΔH (kcal/mol)	[b]K_b (M^{-1})	[c]N	[d]Total helix content (%)	[e]NRMSD	[f]Bound helix content (%)
PspA$_{1-24}$	N/A				9	0.03	
	DOPC	−6.2 ± 0.28	9.1×10^4	76	21	0.05	78
	DOPC/DOPG 8:2	−8.2 ± 0.22	2.6×10^5	39	34	0.02	80
	DOPC/DOPG 6:4	−8.0 ± 0.13	1.7×10^5	25	45	0.04	77
Vipp1$_{1-24}$	N/A				8	0.06	
	DOPC	−3.9 ± 0.18	9.2×10^4	125	12	0.04	42
	DOPC/DOPG 8:2	−7.6 ± 0.21	2.1×10^5	35	39	0.05	91
	DOPC/DOPG 6:4	−8.0 ± 0.17	2.3×10^5	21	50	0.06	77

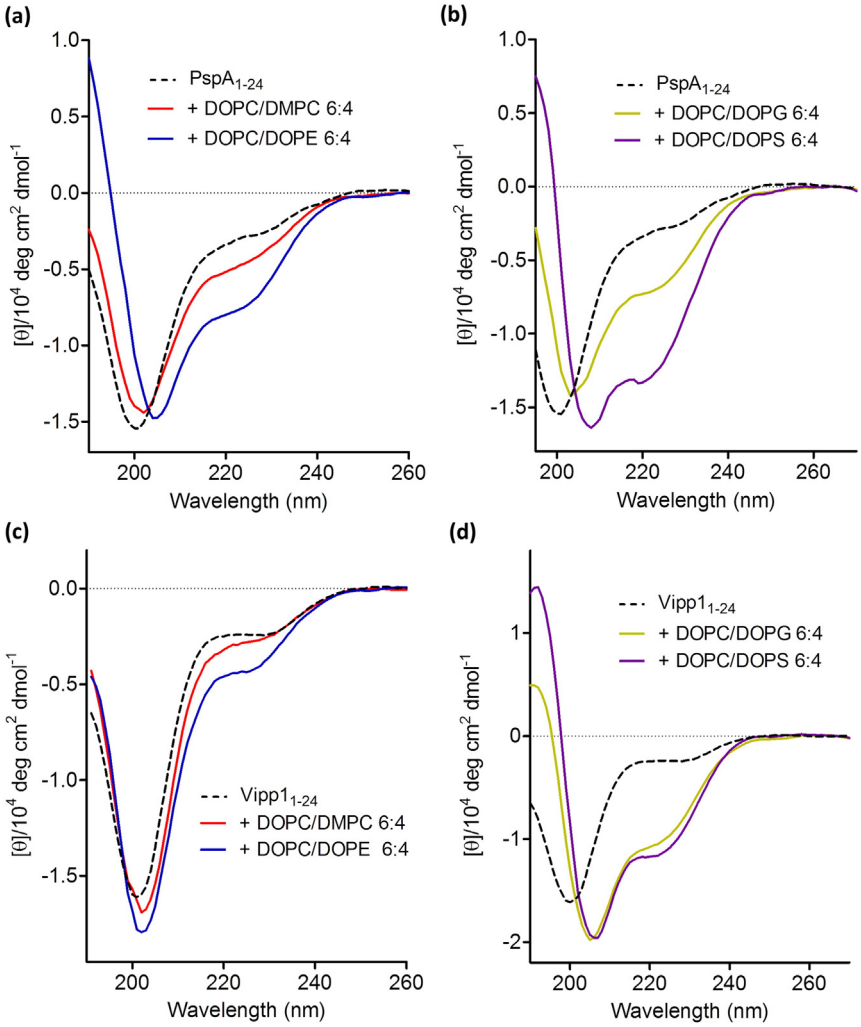

Fig. 4. CD spectra showing spectral effects associated with a disordered-to-helix transition of $PspA_{1-24}$ and $Vipp1_{1-24}$ when incubated with LUVs of different phospholipid compositions. (a) $PspA_{1-24}$ incubated with DOPC/DMPC 6:4 (low SCE stress) and DOPC/DOPE 6:4 (high SCE stress) LUVs. (b) $PspA_{1-24}$ incubated with LUVs containing anionic lipids DOPC/DOPG 6:4 and DOPC/DOPS 6:4. (c) $Vipp1_{1-24}$ incubated with DOPC/DMPC 6:4 (low SCE stress) and DOPC/DOPE 6:4 (high SCE stress) LUVs. (d) $PspA_{1-24}$ incubated with LUVs containing anionic lipids DOPC/DOPG 6:4 and DOPC/DOPS 6:4. The peptide concentration was 300 μM and phospholipid concentration was 4.2 mM.

and Supplementary Table 2). The trend is not linear, with modest increases observed from 10% to 30% DOPG before a large increase is seen between 30% and 40%. A similar trend was observed with DOPC LUVs containing 20% or 40% DOPS (Supplementary Fig. 4c and Supplementary Table 2). Considering the ITC results with $Vipp1_{1-24}$ (see above), this increase in net α-helix content is likely due to both more peptides being associated with the membrane and a higher helical content of those membrane-bound.

The inference that anionic lipid charge density and electrostatic interactions affect $PspA_{1-24}$ and $Vipp1_{1-24}$ membrane binding and structure was also tested by using *E. coli* TLE LUVs. These have high anionic lipid content (over 30%) and more closely represent the native lipid environment of $PspA_{1-24}$ than DOPC-based synthetic vesicles. Notably, Vipp1 N-terminal region comprising $Vipp1_{1-24}$ is required for binding *E. coli* TLE vesicle [18,28]. The CD spectra for both peptides gradually change from an appearance of unordered structure to that of a peptide with increasing helical content as the L/P ratio increases (Fig. 5 and Supplementary Table 1).

A V11E substitution in the hydrophobic face of AHa abolishes PspA IM-binding and formation of high-order oligomeric effectors [19]. Accordingly, a $PspA_{1-24}$ V11E peptide (see Supplementary Fig. 1) did not bind DOPC SUVs in ITC studies (Supplementary Fig. 5a) nor did it display any transition from unordered to helical structure in the presence of LUVs with either high level SCE stress, 40% DOPG or *E. coli* TLE in CD studies (Supplementary Fig. 5b and Supplementary Table 2). The addition of trifluoroethanol (TFE) caused a transition of $PspA_{1-24}$ V11E to a helical structure (Supplementary Fig. 5c). The inability of $PspA_{1-24}$ V11E to gain helicity in the presence of vesicles is therefore not a

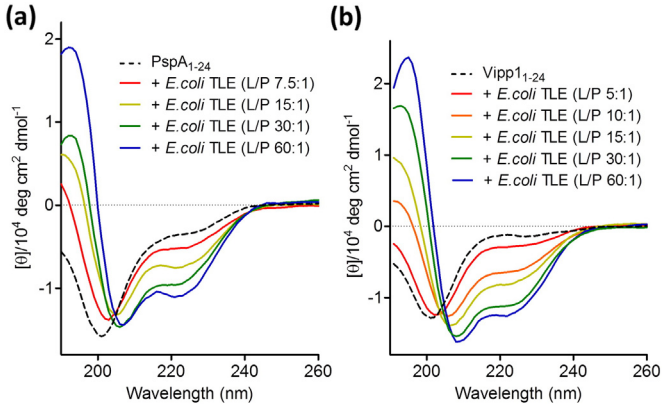

Fig. 5. CD spectra of $PspA_{1-24}$ and $Vipp1_{1-24}$ when incubated with increasing amounts of *E. coli* Total Lipid Extract (TLE) LUVs. (a) $PspA_{1-24}$ incubated at lipid:peptide ratios from 7.5:1 to 60:1. (b) $Vipp1_{1-24}$ incubated at lipid to peptide (L/P) ratios from 5:1 to 60:1. The peptide concentration was 300 μM.

consequence of the V11E substitution itself making a helical structure unfavourable, but rather through failing to bind to vesicles.

3.4. Effect of peptides on LUVs stability

To examine whether $PspA_{1-24}$ and $Vipp1_{1-24}$ peptide binding exerts an effect on membrane stability of vesicles a calcein efflux assay was used to probe leakage. Previously described vesicle compositions (see above) were used to explore if any peptide effects on calcein dye release are modulated by bilayer content. The vesicles bilayer stability was monitored as a function of peptide concentration. The PspA and Vipp1 AHa peptides had no effect on the stability of DOPC vesicles (data not shown) or those with 20% mole fraction DOPG (Fig. 6a). However, at 40% mole fraction DOPG dye leakage was observed starting from a 70:1 L/P ratio (Fig. 6b). The results revealed that PspA and Vipp1 AHa peptides can affect the vesicle structure upon binding and that $Vipp1_{1-24}$ was markedly more effective at causing dye release than $PspA_{1-24}$. $PspA_{1-24}$ V11E did not cause dye release from any vesicle composition (Supplementary Fig. 6a, b). Samples of 40% DOPG vesicles incubated with $Vipp1_{1-24}$ were submitted for EM analysis alongside non-treated vesicles to see if a detrimental effect on the membrane upon peptide binding could be visualised (Fig. 6c). In the presence of $Vipp1_{1-24}$ multiple small spheres measuring around 10–20 nm in diameter are seen. These spheres were not seen in samples containing either vesicles or $Vipp1_{1-24}$ alone (data not shown), thus they are unlikely to result from an intrinsic vesicle instability or peptide aggregation. Instead, they may be micelles caused by detergent like disintegration of the vesicles by the $Vipp1_{1-24}$. To further test this possibility, DLS studies were undertaken on 40% DOPG vesicles in the absence and presence of $Vipp1_{1-24}$ (Fig. 6d). The measured vesicles size distributions showed that 40% DOPG vesicles are all over 50 nm in diameter but when they are incubated with $Vipp1_{1-24}$ a shift to particles with diameters around 10–20 nm is observed, similar in size to the particles seen in the EM images.

The stability of vesicles with low (DMPC/DOPC 4:6) and high (DOPE/DOPC 4:6) SCE stress were probed with $PspA_{1-24}$ and

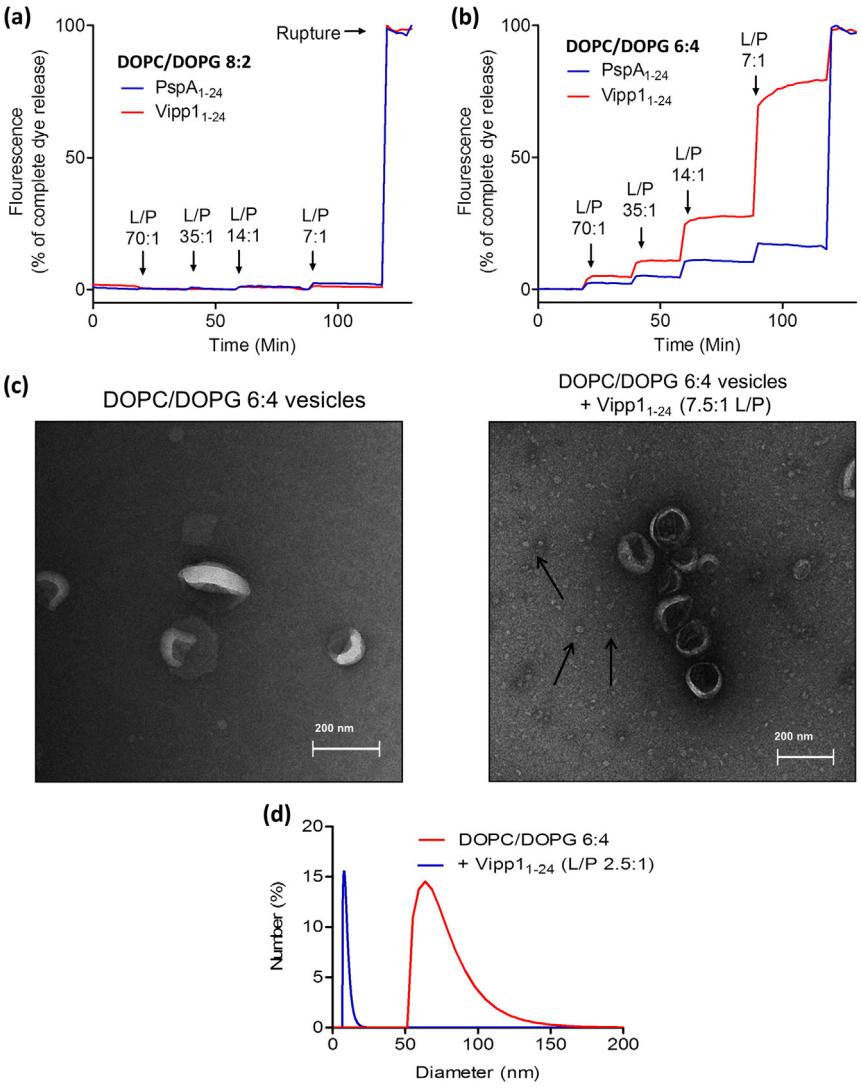

Fig. 6. $PspA_{1-24}$ and $Vipp1_{1-24}$ cause destabilisation of vesicles containing a high proportion of anionic lipids. (a, b) Calcein efflux assays monitoring encapsulated dye release from (a) DOPC/DOPG 8:2 and (b) DOPC/DOPG 6:4 vesicles upon $PspA_{1-24}$ and $Vipp1_{1-24}$ peptide titrations. Fluorescence was measured every 2 min and fluorescence from vesicle and buffer only controls was subtracted. Assays were undertaken using 1 mM lipid concentration and the value for complete dye release was obtained by addition of 2 mM $C_{12}E_8$ to rupture any remaining vesicles. Traces in (a) and (b) are representative examples but trends were preserved in all experiments done (3 repeats with independent vesicle preparations). The error in the final value obtained before vesicle rupture was ± 3% in (a) and ± 9% in (b). (c) Negative stain EM images of DOPC/DOPG 6:4 vesicles alone (left) and incubated with $Vipp1_{1-24}$ at a 7.5:1 lipid to peptide ratio (right). Arrows on the right hand panel indicate the possible formation of micelles. (d) Dynamic light scattering data of 100 nm extruded DOPC/DOPG 6:4 vesicles without or with $Vipp1_{1-24}$ at a 2.5:1 lipid to peptide (L/P) ratio.

Vipp1$_{1-24}$ peptides. The addition of PspA$_{1-24}$ caused moderate dye release exclusively from vesicles with high SCE stress starting from 14:1 L/P ratio (Supplementary Fig. 6c). The Vipp1$_{1-24}$ showed no effect on vesicles stability irrespective of low or high SCE stress (Supplementary Fig. 6d).

Taken together with the results obtained in ITC and CD experiments we now establish that AHa of PspA and Vipp1 is able to sense SCE stress and anionic lipids to directly bind the membrane, affecting both protein and (at least in certain cases) membrane structure.

3.5. Inhibition of PspF activity

The AHb of PspA (residues 25–42) is a putative AH adjacent to AHa (Fig. 1). Notably, the crystal structure of the monomeric PspA$_{1-144}$ fragment which binds to PspF and acts as a negative regulator, includes AHb as a part of the coiled coil [21]. Previous studies strongly suggested a hydrophobic interaction between AHb and the W56 loop of PspF$_{1-275}$ is needed for PspF negative regulation [12,19]. However, the specific nature of the interaction is not characterised and a direct effect of the AHb upon PspF activity was not demonstrated. We used the NADH-coupled ATPase assay to determine if a PspA AHb-derived peptide, PspA$_{25-47}$ (Fig. 1 and Supplementary Fig. 1), can negatively regulate the AAA domain of PspF$_{1-275}$. A 3-fold excess of full length PspA is required for complete inhibition of the PspF$_{1-275}$ ATPase activity [10] and in agreement, equimolar and 2:1 ratios of PspA$_{25-47}$ to PspF$_{1-275}$ had no apparent effect on the ATPase activity of PspF$_{1-275}$ (data not shown). However, at a 5-fold excess of PspA$_{25-47}$ inhibition of ATPase was evident with activity dropping to around 80% that of PspF$_{1-275}$ alone (Fig. 7a). Further increases in PspA$_{25-47}$ concentration gave a linear decrease in ATPase activity until near complete inhibition was achieved at around a 24:1 PspA$_{25-47}$ to PspF$_{1-275}$ M ratio (Fig. 7a, b). However, even at a 50-fold molar excess, PspA$_{25-47}$ was unable to inhibit ATPase activity of PspF$_{1-275}$ W56A (Fig. 7a). To see if inhibition is specific to PspA$_{25-47}$, other PspA peptides were also assayed. PspA$_{1-24}$ is also able to impart a degree of inhibition dependent on the W56 residue of PspF (Fig. 7a), and at a 24-fold excess of PspA$_{1-24}$ over PspF$_{1-275}$ the ATPase activity is reduced to around 40% of PspF$_{1-275}$ alone (Fig. 7a, b). The V11E mutation on the hydrophobic face of PspA$_{1-24}$ strongly diminished the inhibition of PspF$_{1-275}$ ATPase activity (Fig. 7b). Vipp1$_{1-24}$ also repressed the ATPase activity of PspF$_{1-275}$ showing over 20% reductions at a 24-fold excess (Fig. 7b). It appears that a degree of ATPase repression can be obtained by all AH peptides, yet the AHb containing PspA$_{25-47}$ is noticeably the most potent.

4. Discussion

4.1. Influence of membrane stress and composition on AHa helical structure

The results obtained in this work establish that the N-terminal AH of PspA and Vipp1, AHa, is an IM-binding determinant which may act as a membrane stress-sensing AH. The AH mediated membrane sensing trends of the PspA$_{1-24}$ and Vipp1$_{1-24}$ peptides coincide with comparative vesicle-binding levels seen in PspA WT and Vipp1 WT proteins [18]. This provides strong evidence for a direct lipid interaction between the N-terminal AHa of PspA and Vipp1 being responsible for the specific membrane binding. Direct vesicle-binding of both PspA$_{1-24}$ and Vipp1$_{1-24}$ is observed in ITC experiments. The results indicate that increases in the anionic lipid content increase the number of PspA$_{1-24}$ and Vipp1$_{1-24}$ interactions per lipid vesicle. CD spectroscopic studies indicate that the PspA and Vipp1 N-terminal peptides behave similarly to a typical membrane sensing AH [39,40], being unordered in solution and then folding into more helical structures upon membrane association. A V11E mutation of PspA$_{1-24}$ prevents any membrane binding and helix formation irrespective of the tested vesicle composition. Most likely the conserved amphiphilicity of PspA$_{1-24}$ is required for AHa mediated membrane-binding and V11 is part of this helix once membrane associated.

Electrostatics and SCE stress both play a role in the membrane association of PspA$_{1-24}$ and Vipp1$_{1-24}$ AHa. The membrane SCE stress-dependent AHa binding is much more apparent for PspA$_{1-24}$ than Vipp1$_{1-24}$. The same binding trends are seen for PspA and Vipp1 proteins indicating that SCE stress sensing must be directly mediated by the corresponding N-terminal AHa region. In contrast to the SCE stress-sensing trends, Vipp1$_{1-24}$'s membrane association is strongly modulated by anionic lipid content, but the effects on PspA$_{1-24}$ are less pronounced. A large increase in the helix content of membrane-bound Vipp1$_{1-24}$ is also observed when anionic lipids are included in the membrane. Similar increased specificity for negatively charged membranes has been seen for a number of AH peptides including those from N-BAR domains and the N-terminal region of GTPase activating protein RGS4 [41,42].

The differences in SCE stress and anionic lipids sensing between PspA$_{1-24}$ and Vipp1$_{1-24}$ could be explained by their distinct physicochemical properties. PspA$_{1-24}$ has a higher average hydrophobicity than Vipp1$_{1-24}$ (PspA$_{1-24}$ − 0.392 H and Vipp1$_{1-24}$ − 0.245 H). PspA$_{1-24}$ should therefore have a higher avidity for the hydrophobic cavities created by lipid packing defects induced SCE stress, increasing its stress sensing ability in neutral bilayers. AHs such as the ALPS motif that purely sense lipid

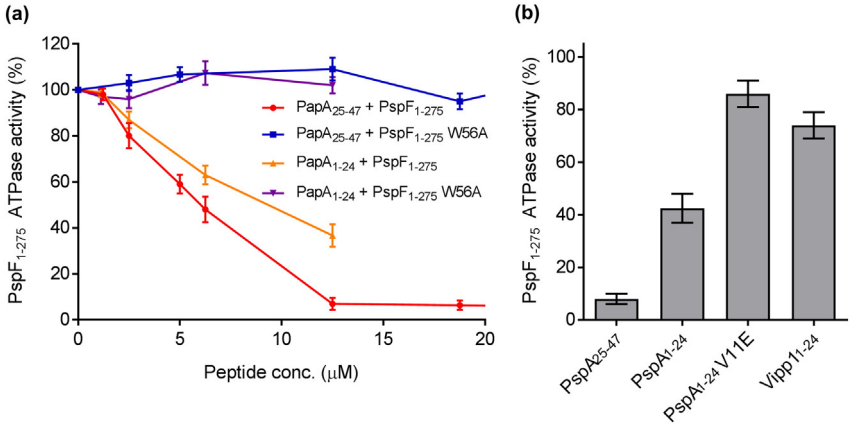

Fig. 7. PspA$_{25-47}$ AHb peptide can inhibit the ATPase activity of PspF, mimicking PspA negative regulatory function. (a) ATPase activity of PspF$_{1-275}$ (and negative control PspF$_{1-275}$ W56A) as a function of increasing concentration of either the PspA$_{25-47}$ or PspA$_{1-24}$. PspF$_{1-275}$ and PspF$_{1-275}$ W56A were used at a final concentration of 0.75 μM in all assays with ATPase activity determined by the NADH-coupled ATP regeneration system. Results are expressed as the percentage of the PspF$_{1-275}$ activity in the absence of the peptides. (b) Bar graph of PspF$_{1-275}$ ATPase activity for all PspA and Vipp1 peptides tested at 12.5 μM (the point at which complete inhibition is seen for PspA$_{25-47}$). The error bars in (a, b) represent the standard error of the mean values from 3 independent measurements.

packing defects caused by SCE stress are typified by their lack of charged residues on the hydrophilic face [39]. Increasing the number of charged residues on the polar face decreases packing defect sensitivity of the AH but increases membrane association through electrostatic interactions [43]. The lower number of charged residues on the polar face of PspA AHa can further explain its enhanced sensitivity for SCE stress dependent binding compared with the Vipp1 AHa. Positively charged residues on the AH encourage interactions with negatively charged lipids, therefore Vipp1's two extra cationic residues will promote its interaction with anionic lipids. This is in full agreement with results obtained with PspA and Vipp1 proteins [18].

4.2. Effect of AHa on membrane stability

The vesicle destabilising properties of the peptides show, for the first time, that binding of the AHa region of PspA and Vipp1 has an effect on the physical state of the membrane. However, the detrimental nature of this interaction seems counterintuitive for a membrane maintenance role of PspA and Vipp1 proteins *in vivo*. Potentially, the PspA and Vipp1 high-order oligomers may function with AHa's regularly and precisely spaced to regularise and limit the number of the contacts that can be made with the membrane. PspA forms a range of oligomers, up to 36-mer, following membrane stress *in vivo* [13,16] and is arranged as a 9-fold symmetry 36-mer ring structure *in vitro* [15]. Indeed, PspA monomers have a high affinity for the IM but no effector function in contrast to the PspA high-order oligomers which do act as effectors [17,19]. Recent data also suggests that although low-order oligomers of Vipp1 have a high affinity for the membrane, it is the high-order oligomeric ring, with lower membrane affinity, that performs as an effector *in vitro* [44]. Notably, the C-terminal tail (HD5) in Vipp1 (see Fig. 1) negatively controls a non-productive association between the Vipp1 high-order oligomeric effectors increasing tolerance against thylakoid membrane stress and suggesting single Vipp1 ring structure are a functional unit [45]. Therefore, an upper size limited and likely ring shaped high-order assembly of PspA or Vipp1 could provide a sufficient density of membrane binding AHa's to insert into the hydrophobic cavities arising from lipid packing defects and relax the resulting membrane SCE stress (see Fig. 8a, b). This mechanism could act to stabilise stressed membranes while preventing bilayer carpeting and the resulting detergent like disintegration through an overwhelming of the membrane with AHa's. Lipid packing defects and accumulation of membrane SCE stress can specifically influence the structure and activity of peripheral membrane proteins by providing energetically favourable sites for membrane binding often changing conformation and the oligomeric state of a protein [46]. The insertion of AHs into a lipid bilayer can then result in a decrease of SCE stress [46,47] and so this may be one function of the AHa's of PspA and Vipp1 when acting as high-order oligomeric effectors.

4.3. Role of AHb in negative control

Here we also demonstrated that the $PspA_{25–47}$ peptide containing AHb specifically represses $PspF_{1–275}$ ATPase activity. Results showing that the ATPase activity of a $PspF_{1–275}$ W56A mutant cannot be suppressed by $PspA_{25–47}$ demonstrate that the peptide is likely using the same inhibition mechanism as the full length PspA through contacting the W56 loop of PspF [3,10,12]. Although the PspA AHa and even the Vipp1 AHa peptide are able to decrease the ATPase activity, $PspA_{25–47}$ is by far the most effective inhibitor suggesting that an AHb conserved sequence might be specifically required for this functionality. The tested peptides share an amphipathic nature when in an α-helical conformation so hydrophobic interactions between the apolar face of the AHb and the W56 loop of PspF could be a prime interaction candidates for the ATPase inhibition. Indeed, the substitution of V29 with charged residue on the hydrophobic face of AHb abolishes interactions and negative control of PspF [19] while an E37A substitution of the charged residue on the opposite face of AHb, has only moderate effect on ATPase inhibition and no effect on the binding interaction with PspF [21]. Full length PspA is much more effective at repressing $PspF_{1–275}$ than the $PspA_{25–47}$ peptide. A 24-fold molar excess of $PspA_{25–47}$ is required for complete $PspF_{1–275}$ ATPase inhibition, but, in similar assays only a three-fold excess of full length PspA can cause the same level of inhibition [10]. PspA and $PspF_{1–275}$ demonstrate a strong propensity to self-assemble into a single defined heteromeric regulatory complex but isolated PspA helical domains (HDs) have a low affinity for $PspF_{1–275}$ [10]. Considering that PspA residues 69–186 also contribute to negative control of $PspF_{1–275}$ [10], it is likely that PspA makes multiple interactions with $PspF_{1–275}$ which co-operate to form a tightly bound complex where the AHb region is in the correct location to directly associate with the W56 loop. This is clearly not the case for the $PspA_{25–47}$ peptide where only a single interaction with the W56 loop is possible. The binding affinity of the peptide for $PspF_{1–275}$ will therefore be much lower than PspA WT and a much higher concentration of the peptide will be required for a similar level of ATPase inhibition.

4.4. An integrated perspective

Taken together, our results imply that the PspA N-terminal AHa is directly responsible for membrane association and effector function while the AHb directly imposes inhibition of PspF's ATPase activity and negative control. The AHa region is unordered in a monomeric form of PspA acting as a negative regulator [21] and we show here that upon membrane interaction the PspA AHa peptide undergoes a transition to an ordered helical structure. Considering that AHa and AHb are located adjacent to one another separated by a conserved proline residue in the primary sequence of full length PspA, some steric hindrance or structural remodelling following membrane binding could prevent concurrent association to PspF and the bilayer (see Fig. 8a, c). A molecular structure of membrane-bound PspA would help to address the cause for the inferred discordant use of AHa or AHb.

We propose that the SCE stress which elicits PspA vesicle binding via AHa relates a physical membrane state to the physiological membrane stress *in vivo*. It is challenging to quantitatively measure the changes in membrane SCE stress *in vivo*, still, severe *psp*-inducing stimuli such as hyperosmotic, ethanol and extreme temperature shocks can affect the lipid packing and so may induce accumulation of SCE stress. The same but to a lesser extent may be true for the PspB-C-dependent *psp*-inducing stimuli such as defects in protein translocation or mislocalisation of type II or III systems secretins.

Maintaining particular membrane mechanical properties upon extracytoplasmic stress may be vital for PspA to support pmf-dependent cellular processes as well as for the roles of PspA in the virulence and antimicrobial resistance of bacteria. The Psp system and PspA proteins determinants such as AHa are potential targets for the development of antimicrobials and-or attenuated vaccines against enterobacteria and other pathogenic Gram-negative or Gram-positive bacteria and *Mycobacterium tuberculosis*. In addition, the PspA AHb-based peptide(s) might directly inhibit the Psp response in enterobacteria.

The Vipp1 AHa peptide possesses increased binding and membrane disrupting properties for vesicles with high anionic lipid content (not seen for PspA AHa). Thylakoid and cytoplasmic membranes contain around 25% anionic lipids, lower than the 30–40% threshold that appears to promote an increase in Vipp1 AHa membrane binding sites and the concurrent membrane destabilisation. If this same functionality is conserved in full length Vipp1, then any membrane disrupting properties seem unlikely to be imposed on most of the membrane. Rather, the AHa could selectively target areas with elevated levels of anionic lipids. This modality does not provide obvious benefits in terms of a maintenance function but in terms of thylakoid biogenesis this sensing could be vital. Indeed our findings are in line with a proposed role for Vipp1 in trafficking PG to the thylakoid membrane [48]. Vipp1 may target areas of the cytoplasmic membrane enriched in anionic lipids, such as the site of their synthesis, through AHa mediated association. The

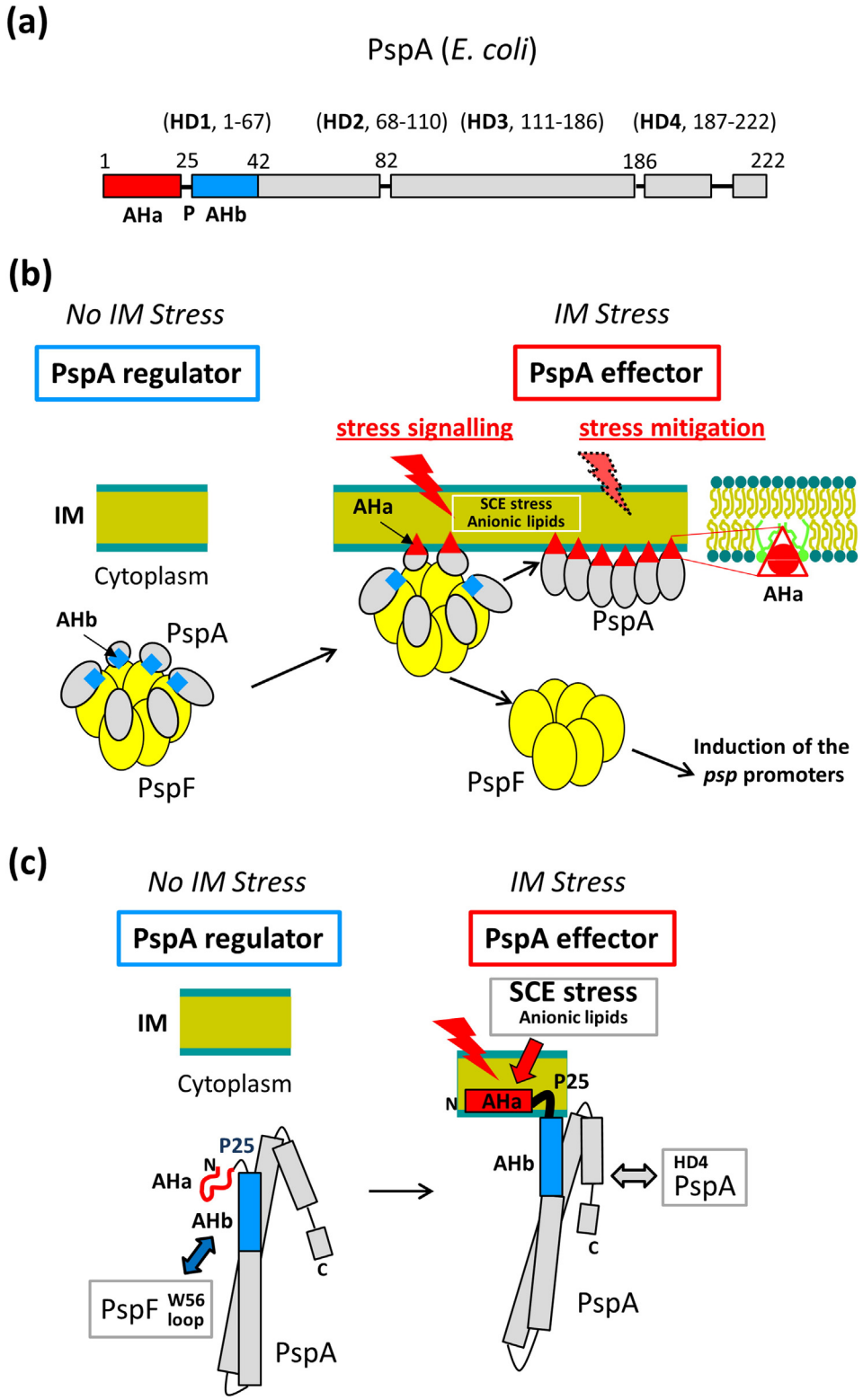

Fig. 8. Model of the N-terminal amphipathic helices AHb and AHa in their respective regulatory and effector functions in PspA. (a) Schematic presentation of the PspA (residues 1–222) α-helices (squares) based on combined $PspA_{1-144}$ crystal structure [21] and the PspA α-helical structure as modelled using Rosetta ab initio folding protocol. In parentheses is the PspA helical structure (HD1–4) as presented in Fig. 1; HD1 is required for membrane binding, HD1–3 are implicated in negative control while HD1 and HD4 are both required for high-order oligomer formation [10,19]; Red square — AHa, Amphipathic Helix a; Blue square — AHb, Amphipathic Helix b; P, residue Proline 25. (b) Under non-stress conditions monomeric PspA imposes negative control upon PspF through interactions mainly *via* AHb. Under IM-stress conditions which increase the SCE stress, PspA either interacts with PspB-C to release PspF and bind the IM or directly binds the IM *via* its AHa leading to release of PspF from the PspA-PspF inhibitory complex. This enables PspA to form IM-bound high-order oligomers that mitigate the IM stress by relaxing SCE stress *via* multiple AHa insertions (far right, AHa, red circle/triangle). The engagement of AHa in membrane binding prevents any further PspA interactions with PspF. PspA, in grey; PspF, in yellow; AHa, red triangle; AHb, blue square. (c) Under non stress conditions the hydrophobic face of AHb of PspA interacts with the hydrophobic W56 loop of PspF inhibiting PspF ATPase activity. The AHa is structurally unordered when PspA is acting as a negative regulator. Under IM-stress conditions PspA senses the increased SCE stress *via* AHa and binds the IM. AHa-IM association causes unordered-to-helical structure transition of AHa. Then the AHa *via* P25 imposes constraints on AHb that disable further interactions of PspA with PspF and lead to PspA oligomerisation through the C-terminal (HD4) region.

high density of AHa insertions of a Vipp1 high-order oligomer could induce local membrane disruption resulting in formation of Vipp1-lipid complexes enriched in PG. Vipp1 could then deliver these lipids by interacting with Alb3.2 located in the thylakoid membrane [49]. Potentially Vipp1 could undertake a membrane maintenance function based on its SCE stress sensing properties, and a role in thylakoid biogenesis through its anionic lipid binding determinant.

Competing financial interests

The authors declare no competing financial interests.

Authors contributions

CM, GJ, OC and MB conceived and designed experiments. CM performed experiments. CM, GJ, OC and MB analysed the experiments. CM and BAW designed, performed and analysed the CD experiments. GJ, CM and MB wrote the paper. CM prepared the figures. All authors reviewed the results and approved the submitted version of the manuscript.

Conflict of Interest

The authors declare that they have no conflicts of interest.

Transparency document

The Transparency document associated with this article can be found, in the online version.

Acknowledgements

This work was funded by the Leverhulme Trust Research project grant RPG-2012-705, the EPSRC *via* grant EP/G00465X/1, by grant J019135 from the UK BBSRC to BAW, and by an EPSRC Centre for Doctoral Training Studentship from the Institute of Chemical Biology (Imperial College London) awarded to CM. We would like to thank Dr. Harry H. Low (Imperial College London) for the help with EM experiments. We would like to thank members of the M. Buck laboratory for critical reading and comments on the manuscript.

Appendix A. Supplementary data

Supplementary data to this article can be found online at doi:10.1016/j.bbamem.2016.10.018.

References

[1] P. Model, G. Jovanovic, J. Dworkin, The *Escherichia coli* phage-shock-protein (*psp*) operon, Mol. Microbiol. 24 (1997) 255–261.
[2] A.J. Darwin, The phage-shock-protein response, Mol. Microbiol. 57 (2005) 621–628.
[3] N. Joly, C. Engl, G. Jovanovic, M. Huvet, T. Toni, X. Sheng, M.P. Stumpf, M. Buck, Managing membrane stress: the phage shock protein (Psp) response, from molecular mechanisms to physiology, FEMS Microbiol. Rev. 34 (2010) 797–827.
[4] J. Flores-Kim, A.J. Darwin, The phage shock protein response, Annu. Rev. Microbiol. 70 (2016) 83–101.
[5] G. Rowley, M. Spector, J. Kormanec, M. Roberts, Pushing the envelope: extracytoplasmic stress responses in bacterial pathogens, Nat. Rev. Microbiol. 4 (2006) 383–394.
[6] A.J. Darwin, Stress relief during host infection: the phage shock protein response supports bacterial virulence in various ways, PLoS Pathog. 9 (2013), e1003388.
[7] P. Datta, J. Ravi, V. Guerrini, R. Chauhan, M.B. Neiditch, S.S. Shell, S.M. Fortune, B. Hancioglu, O.A. Igoshin, M.L. Gennaro, The Psp system of *Mycobacterium tuberculosis* integrates envelope stress-sensing and envelope-preserving functions, Mol. Microbiol. 97 (2015) 408–422.
[8] R.M. Armstrong, K.L. Adams, J.E. Zilisch, D.J. Bretl, H. Sato, D.M. Anderson, T.C. Zahrt, Rv2744c is a PspA ortholog that regulates lipid droplet homeostasis and non-replicating persistence in *Mycobacterium tuberculosis*, J. Bacteriol. 198 (2016) 1645–1661.
[9] N. Zhang, G. Jovanovic, C. McDonald, O. Ces, X. Zhang, M. Buck, Transcripiton regulation and membrane stress management in enterobacterial pathogens, in: M.C. Leake (Ed.), Biophysics of Infection, Advances in Experimental Medicine and Biology, Springer International Publishing, Switzerland 2016, pp. 207–230.
[10] N. Joly, P.C. Burrows, C. Engl, G. Jovanovic, M. Buck, A lower-order oligomer form of phage shock protein A (PspA) stably associates with the hexameric AAA(+) transcription activator protein PspF for negative regulation, J. Mol. Biol. 394 (2009) 764–775.
[11] P. Mehta, G. Jovanovic, T. Lenn, A. Bruckbauer, C. Engl, L. Ying, M. Buck, Dynamics and stoichiometry of a regulated enhancer-binding protein in live *Escherichia coli* cells, Nat. Commun. 4 (2013) 1997.
[12] N. Zhang, T. Simpson, E. Lawton, P. Uzdavinys, N. Joly, P.C. Burrows, M. Buck, A key hydrophobic patch identified in an AAA(+) protein essential for its *in trans* inhibitory regulation, J. Mol. Biol. 425 (2013) 2656–2669.
[13] G. Jovanovic, P. Mehta, L. Ying, M. Buck, Anionic lipids and the cytoskeletal proteins MreB and RodZ define the spatio-temporal distribution and function of membrane stress controller PspA in *Escherichia coli*, Microbiol.-sgm 160 (2014) 2374–2386.
[14] S. Yamaguchi, D.A. Reid, E. Rothenberg, A.J. Darwin, Changes in Psp protein binding partners, localization and behaviour upon activation of the *Yersinia enterocolitica* phage shock protein response, Mol. Microbiol. 87 (2013) 656–671.
[15] B.D. Hankamer, S.L. Elderkin, M. Buck, J. Nield, Organization of the AAA(+) adaptor protein PspA is an oligomeric ring, J. Biol. Chem. 279 (2004) 8862–8866.
[16] T. Lenn, C.N. Gkekas, L. Bernard, C. Engl, G. Jovanovic, M. Buck, L. Ying, Measuring the stoichiometry of functional PspA complexes in living bacterial cells by single molecule photobleaching, Chem. Commun. 47 (2011) 400–402.
[17] R. Kobayashi, T. Suzuki, M. Yoshida, *Escherichia coli* phage-shock protein A (PspA) binds to membrane phospholipids and repairs proton leakage of the damaged membranes, Mol. Microbiol. 66 (2007) 100–109.
[18] C. McDonald, G. Jovanovic, O. Ces, M. Buck, Membrane stored curvature elastic stress modulates recruitment of maintenance proteins PspA and Vipp1, MBio 6 (2015), e01188–15.
[19] G. Jovanovic, P. Mehta, C. McDonald, A. Davidson, P. Uzdavinys, L. Ying, M. Buck, The N-terminal amphipathic helices determine regulatory and effector functions of Phage shock protein A (PspA) in *Escherichia coli*, J. Mol. Biol. 426 (2014) 1498–1511.
[20] S.L. Elderkin, P. Bordes, S. Jones, M. Rappas, M. Buck, Molecular determinants for PspA-mediated repression of the AAA transcriptional activator PspF, J. Bacteriol. 187 (2005) 3238–3248.
[21] H. Osadnik, M. Schopfel, E. Heidrich, D. Mehner, H. Lilie, C. Parthier, H.J. Risselada, H. Grubmuller, M.T. Stubbs, T. Bruser, The PspF-binding domain PspA and the PspA.F complex: new insights into the coiled-coil dependent regulation of AAA+ proteins, Mol. Microbiol. 98 (2015) 743–759.
[22] U.C. Vothknecht, S. Otters, R. Hennig, D. Schneider, Vipp1: a very important protein in plastids?! J. Exp. Bot. 63 (2012) 1699–1712.
[23] L. Zhang, W. Sakamoto, Possible function of VIPP1 in thylakoids: protection but not formation? Plant Signal. Behav. 8 (2013), e22860.
[24] S.J. Bryan, N.J. Borroughs, D. Shevela, J. Yu, L.-N.L. Rupprecht, G. Mastroianni, Q. Xue, I. Llorente-Garcia, M.C. Leake, L.A. Eichacker, D. Schneider, P.J. Nixon, C.W. Mullineaux, Localisation and interactions of the Vipp1 protein in cyanobacteria, Mol. Microbiol. 94 (2014) 1179–1195.
[25] L. Zhang, W. Sakamoto, Possible function of Vipp1 in maintaining chloroplast membranes, Biochim. Biophys. Acta 1847 (2015) 831–837.
[26] E. Aseeva, F. Ossenbühl, L.A. Eichacker, G. Wanner, J. Soll, U.C. Vothnecht, Complex formation of Vipp1 depends on it's α-helical PspA-like domain, J. Biol. Chem. 279 (2004) 35535–35541.
[27] M.P. DeLisa, P. Lee, T. Palmer, G. Georgiou, Phage shock protein PspA of *Escherichia coli* relieves saturation of protein export *via* the Tat pathway, J. Bacteriol. 186 (2004) 366–373.
[28] S. Otters, P. Braun, J. Hubner, G. Wanner, U.C. Vothknecht, F. Chigri, The first alpha-helical domain of the vesicle-inducing protein in plastids 1 promotes oligomerization and lipid binding, Planta 237 (2013) 529–540.
[29] R. Hennig, J. Heidrich, M. Saur, L. Schmuser, S.J. Roeters, N. Hellmann, S. Woutersen, M. Bonn, T. Weidner, J. Markl, D. Schneider, IM30 triggers membrane fusion in cyanobacteria and chloroplasts, Nat. Commun. 6 (2015) 7018.
[30] J.G. Lees, B.R. Smith, F. Wien, A.J. Miles, B.A. Wallace, CDtool-an integrated software package for circular dichroism spectroscopic data processing, analysis, and archiving, Anal. Biochem. 332 (2004) 285–289.
[31] L. Whitmore, B.A. Wallace, Protein secondary structure analyses from circular dichroism spectroscopy: methods and reference databases, Biopolymers 89 (2008) 392–400.
[32] S.W. Provencher, J. Glöckner, Estimation of globular protein secondary structure from circular dichroism, Biochemistry 20 (1981) 33–37.
[33] I.H. van Stokkum, H.J. Spoelder, M. Bloemendal, R. van Grondelle, F.C. Groen, Estimation of protein secondary structure and error analysis from circular dichroism spectra, Anal. Biochem. 191 (1990) 110–118.
[34] N. Joly, J. Schumacher, M. Buck, Heterogeneous nucleotide occupancy stimulates functionality of phage shock protein F, an AAA+ transcriptional activator, J. Biol. Chem. 281 (2006) 34997–35007.
[35] J.G. Nørby, Coupled assay of Na+, K+ATPase activity, Methods Enzymol. 156 (1988) 116–119.
[36] S.S. Chong, S.G. Taneva, J.M. Lee, R.B. Cornell, The curvature sensitivity of a membrane-binding amphipathic helix can be modulated by the charge on a flanking region, Biochemistry 53 (2014) 450–461.
[37] B. Nucher, Alpha-synuclein has a high affinity for packing defects in a bilayer membrane: a thermodynamics study, J. Biol. Chem. 279 (2004) 21966–21975.
[38] T. Wieprecht, M. Beyermann, J. Seelig, Thermodynamics of the coil-alpha-helix transition of amphipathic peptides in a membrane environment: the role of vesicle curvature, Biophys. Chem. 96 (2002) 191–201.
[39] G. Drin, B. Antonny, Amphipathic helices and membrane curvature, FEBS Lett. 584 (2010) 1840–1847.

[40] G. Drin, J.F. Casella, R. Gautier, T. Boehmer, T.U. Schwartz, B. Antonny, A general amphipathic alpha-helical motif for sensing membrane curvature, Nat. Struct. Mol. Biol. 14 (2007) 138–146.
[41] F. Fernandes, L.M. Loura, F.J. Chichon, J.L. Carrascosa, A. Fedorov, M. Prieto, Role of helix 0 of the N-BAR domain in membrane curvature generation, Biophys. J. 94 (2008) 3065–3073.
[42] L.S. Bernstein, A.A. Grillo, S.S. Loranger, M.E. Linder, RGS4 binds to membranes through an amphipathic alpha-helix, J. Biol. Chem. 275 (2000) 18520–18526.
[43] M.B. Jensen, V.K. Bhatia, C.C. Jao, J.E. Rasmussen, S.L. Pedersen, K.J. Jensen, R. Langen, D. Stamou, Membrane curvature sensing by amphipathic helices: a single liposome study using alpha-synuclein and annexin B12, J. Biol. Chem. 286 (2011) 42603–42614.
[44] J. Heidrich, V. Wulf, R. Hennig, M. Saur, J. Markl, C. Sönnichsen, D. Schneider, Organization into higher-ordered ring structures counteracts membrane binding of IM30, a protein associated with inner membranes in chloroplasts and cyanobacteria, J. Biol. Chem. (2016), http://dx.doi.org/10.1074/jbc.M116.722686.
[45] L. Zhang, H. Kondo, H. Kamikubo, M. Kataoka, W. Sakamoto, VIPP1 has a disordered C-terminal tail necessary for protecting photosynthetic membranes against stress in *Arabidopsis*, Plant Physiol. (2016), http://dx.doi.org/10.1104/pp.16.00532.
[46] E. van den Brink-van der Laan, J.A. Killian, B. de Kruijff, Nonbilayer lipids affect peripheral and integral membrane proteins *via* changes in the lateral pressure profile, Biochim. Biophys. Acta 1666 (2004) 275–288.
[47] L. Iversen, S. Mathiasen, J.B. Larsen, D. Stamou, Membrane curvature bends the laws of physics and chemistry, Nat. Chem. Biol. 11 (2015) 822–825.
[48] A. Nordhues, M.A. Schottler, A.K. Unger, S. Geimer, S. Schonfelder, S. Schmollinger, M. Rutgers, G. Finazzi, B. Soppa, F. Sommer, T. Muhlhaus, T. Roach, A. Krieger-Liszkay, H. Lokstein, J.L. Crespo, M. Schroda, Evidence for a role of VIPP1 in the structural organization of the photosynthetic apparatus in Chlamydomonas, Plant Cell 24 (2012) 637–659.
[49] V. Gohre, F. Ossenbuhl, M. Crevecoeur, L.A. Eichacker, J.D. Rochaix, One of two Alb3 proteins is essential for the assembly of the photosystems and for cell survival in Chlamydomonas, Plant Cell 18 (2006) 1454–1466.
[50] R. Gautier, D. Douguet, B. Antonny, G. Drin, HELIQUEST: a web server to screen sequences with specific alpha-helical properties, Bioinformatics 24 (2008) 2101–2102.